eXPRESS Polymer Letters Vol.15, No.10 (2021) 957–971
Available online at www.expresspolymlett.com
https://doi.org/10.3144/expresspolymlett.2021.77

Synthesis and characterization of polyacrylonitrile-grafted copolymers based on poly(vinylidene fluoride)

A. D. Khudyshkina, Yu. N. Luponosov, V. G. Shevchenko, S. A. Ponomarenko*

Enikolopov Institute of Synthetic Polymeric Materials of the Russian Academy of Sciences, Moscow, Russia

Received 23 March 2021; accepted in revised form 3 June 2021

Abstract. Grafted poly(vinylidene fluoride) (PVDF)-based copolymers attract great attention due to their tunable ferroelectric and dielectric characteristics, which gives great perspectives for electronic applications. In this work, two strategies for polyacrylonitrile-grafted PVDF-based copolymers synthesis, namely single electron transfer radical polymerization (SET-LRP) and photoinduced Cu(II)-mediated reversible deactivation radical polymerization (RDRP) were investigated, their advantages and shortcomings are discussed. Using these methods two series of poly(vinylidene fluoride-*co*-chlorotrifluoroethylene)-grafted-polyacrylonitrile p(VDF-*co*-CTFE)-*g*-PAN and poly(vinylidene fluoride-*co*-trifluoroethylene-*co*-chlorotrifluoroethylene)-grafted-polyacrylonitrile p(VDF-*co*-TrFE-*co*-CTFE)-*g*-PAN with different PAN content were prepared. Important characteristics of the grafted PVDF-based copolymers such as phase behavior, thermal stability, and dielectric properties were investigated, and impacts of the macromolecular backbone type, as well as the content of grafted PAN on these properties, are discussed. It was shown that PAN incorporation leads to significant dielectric properties change since the dielectric permittivity of PAN-grafted copolymers is twice higher in comparison to the pristine copolymers. The crucial impact of PAN grafting onto PVDF-based copolymers backbone on their phase, thermal and dielectric behavior is demonstrated.

Keywords: *polymer synthesis, molecular engineering, fluoropolymer, poly(vinylidene fluoride)-based copolymers, grafted polymer, ATRP polymerization*

1. Introduction

Fluoropolymers based on poly(vinylidene fluoride) (PVDF) attract great interest from researchers due to the wide range of their applications [1–6]. First of all, PVDF-based polymers have a large number of useful properties such as high thermal and chemical resistance, hydrolytic stability, resistance to oxidation as well as both oil and water repellency because of low surface energy [1, 3, 7–9]. In fact, this great range of properties is owing to the special characteristics of a fluorine atom. Both high ionization potential and low polarizability of fluorine atoms lead to low surface energy and low refractive index for perfluorocarbons, while high electronegativity provides strong C–F bond energy (485 kJ/mol) of PVDF-based macromolecules [2, 10].

Furthermore, it was reported that PVDF is the most perspective ferroelectric polymer applied for a broad range of electronic applications such as electromechanical and acoustic transducers, artificial organs, memory devices, *etc.* [11–14]. In fact, PVDF is typically a crystalline polymer having five crystal polymorphs named α, β, γ, δ, ε, where the β-phase is more significant due to its piezo-, pyro- and ferroelectric properties [15, 16]. It is well known that the standard techniques for PVDF films obtaining from solution or melt lead to producing of the polymer with the α-phase. The polar crystalline β-phase can be obtained by post-treatment of α-PVDF films using annealing at elevated temperatures [17–19], poling in a high electric field, mechanical stretching, or quenching techniques. However, the techniques

*Corresponding author, e-mail: luponosov@ispm.ru

mentioned above are not only technologically disadvantageous but often inapplicable for other materials comprised in electronic devices based on PVDF. Despite several novel techniques of β-phase production (such as direct crystallization of β-PVDF from melt upon an ionic liquid [20], UV-induced transformation of α- to β-phase of PVDF [21]) were reported recently, application of PVDF as piezo- and ferroelectric polymer still remains a challenge of great interest.

To overcome difficulties of the β-phase production, different copolymers based on PVDF have been proposed. The most known PVDF-based copolymer is poly(vinylidene fluoride-*co*-trifluoroethylene) (p(VDF-*co*-TrFE)) which has a great advantage over traditional PVDF. Wang *et al*. [22] reported that even non-annealed p(VDF-*co*-TrFE) demonstrates normal ferroelectric behavior confirmed by a typical ferroelectric hysteresis loop. Despite the obvious technological advantage of p(VDF-*co*-TrFE), it should be noted that its synthesis includes both a deep hazard and a high cost of the TrFE monomer. To exclude TrFE monomer usage, the controlled hydrogenation of poly(vinylidene fluoride-*co*-chlorotrifluoroethylene) (p(VDF-*co*-CTFE)) can be applied to obtain the well-known PVDF-based terpolymer poly(vinylidene fluoride-*co*-trifluoroethylene-*co*-chlorotrifluoroethylene) (p(VDF-*co*-TrFE-*co*-CTFE)) [23, 24]. Depending on the molar ratio of VDF, TrFE and CTFE units, p(VDF-*co*-TrFE-*co*-CTFE) can demonstrate efficient ferroelectric behavior [24]. Meanwhile, it has been reported that those terpolymers have some shortcomings, such as high dielectric losses, low energy density, and low energy efficiency [25–29]. Besides, the other PVDF-based copolymer is p(VDF-*co*-CTFE), which demonstrates lower spontaneous polarization compared to p(VDF-*co*-TrFE) and p(VDF-*co*-TrFE-*co*-CTFE) copolymers [30]. On the other hand, p(VDF-*co*-CTFE) seems to be not completely investigated copolymer since its ferroelectric behavior has been reported in just a few publications. Thus, the studying of p(VDF-*co*-CTFE)-based copolymers ferroelectric and dielectric behavior is an actual scientific task. The required dielectric properties such as high dielectric constant, low dielectric loss, high energy efficiency, and stable residual polarization at elevated temperatures, and low operating voltages are crucial challenges to be solved in this field.

To expand the range of PVDF-based copolymers applications and tune their ferroelectric characteristics, a grafted copolymer concept can be utilized [25–29, 31–34]. The promising approach seems to be a grafting of a polar monomer onto a PVDF-based backbone. One can expect that the incorporation of polar functional groups could enhance the polarity of the macromolecule and promote the increase of the dielectric constant [35].

The most developed method of graft copolymers synthesis is an atom transfer radical polymerization (ATRP) [36–39]. Generally, ATRP process is mediated by a transition metal complex, which is responsible for the splitting of C–Cl bonds and further macro-radicals generation. Since ATRP requires a relatively high concentration of metal catalyst (about 1000–10 000 ppm) [27], the metal ions contamination in resulting grafted copolymers can significantly affect their dielectric and ferroelectric properties. Taking this into account, several methodologies of ATRP were developed to reduce the concentration of the metal catalyst [40]. One of them is a single electron transfer – living radical polymerization (SET-LRP) process initiated by a trace amount of Cu(0)/N-containing ligand system. The first work about successful synthesis of PAN-grafted PVDF-based copolymers via SET-LRP process was reported by Hu *et al.* [41]. Controlled polymerization of p(VDF-*co*-CTFE)-*g*-PAN with different content of grafted PAN was observed, the structure of resultant copolymers was confirmed, and their thermal properties were characterized. Another convenient method to synthesize PAN grafted PVDF-based copolymers is the utilization of photoinduced Cu(II)-mediated reversible deactivation radical polymerization (RDRP). It has been shown that RDRP method allows both to decrease the catalytic metal concentration and simply control the content of grafted PAN by varying the reaction time [42, 43]. Thus, RDRP process is a technologically more perspective method since it implies the preparation of the grafted copolymer with a certain content of incorporated polymer and further investigation of correlations between its structure and properties. However, neither dielectric nor ferroelectric properties of the PAN-grafted copolymers based on PVDF were reported up to now, which seems to be a flaw considering the perspectives of their electronic applications.

Therefore, grafted PVDF-based copolymers are of great interest owing to the advantages of gaining macromolecular compounds with tunable ferroelectric and dielectric characteristics. However, only a

few grafted PVDF-based copolymers are synthesized and characterized so far, which does not allow elucidating the structure-properties relationship for this class of materials and limits the development of the materials with optimal characteristics. Thus, synthesis and comprehensive investigation of thermal properties, phase behavior, solubility, dielectric and ferroelectric characteristics of novel grafted PVDF-based copolymers with different nature and content of incorporated grafted chains are of great importance. The structure-property correlation will certainly allow predicting the properties of developing grafted copolymers and obtain materials with required dielectric and ferroelectric characteristics.

Meanwhile, PAN-grafted PVDF-based copolymers with described dielectric and ferroelectric performance characteristics have not yet been reported. In this work, two strategies (SET-LRP and UV-induced RDRP methods) of p(VDF-*co*-CTFE)-*g*-PAN and p(VDF-*co*-TrFE-*co*-CTFE)-*g*-PAN synthesis were employed to prepare copolymers with varied content of grafted PAN. These methods of grafted PVDF-based copolymers preparation were compared, their advantages and shortcomings were discussed. For the first time, dielectric properties of p(VDF-*co*-CTFE)-*g*-PAN and p(VDF-*co*-TrFE-*co*-CTFE)-*g*-PAN copolymers were investigated. The PAN grafting onto PVDF-based copolymers backbone leads to crucial dielectric properties changes since the dielectric constant of the grafted copolymers was twice enhanced as compared to the pristine copolymers.

2. Experimental section

2.1. Characterization

^{1}H NMR spectra were recorded on a 'Bruker WP-250 SY' spectrometer at the frequency of 250.13 MHz applying DMSO-d_6 signal (2.49 ppm) as the internal standard. ^{19}F NMR spectra were recorded on a 'Bruker WP-250 SY' spectrometer at the frequency of 282 MHz. In the case of ^{1}H NMR spectroscopy, the samples were analyzed in the form of 2% solutions in DMSO-d_6. In the case of ^{19}F NMR spectroscopy, the samples were analyzed in the form of 8% solutions in DMSO-d_6. The spectra were processed on the computer utilizing the ACD Labs software.

Thermogravimetric analysis (TGA) was carried out in dynamic mode at the temperature range of 50÷700 °C using Mettler Toledo TG50 system equipped with M3 microbalance. The samples were heated at the rate of 10 °C/min in the air and nitrogen atmosphere. Mettler Toledo DSC30 system was used for differential scanning calorimetric (DSC) analysis. The samples were heated at the rate of 10 °C/min at the temperature range of 20÷200 °C.

Novocontrol Alpha-A impedance analyzer with a ZGS Alpha Active Sample Cell and gold-plated disc electrodes 20 mm in diameter was used for room temperature dielectric measurements of permittivity, dielectric loss, and conductivity. The frequency of measurements was changed in the range 0.1–106 c/s; the voltage applied to the electrodes was 1 V. The thickness of the samples was measured by a micrometer with a resolution of 2 microns and averaged over the electrode area.

2.2. Materials

P(VDF-*co*-CTFE) and p(VDF-*co*-TrFE-*co*-CTFE) copolymers (containing 9 and 7 mol% of CTFE, respectively) were provided by PolyK Technologies, State College, PA, USA. Cu(0) powder (99,9%), copper(II) chloride dihydrate (99+%) and 2,2′-bipyridine (99+%) were purchased from Acros Organics B.V.B.A. Tris(2-dimethylaminoethyl)amine (99%) was provided by Abcr GmbH. Acrylonitrile (99+%) was purchased from Acros Organics B.V.B.A. and distilled under an inert atmosphere before used. Dimethyl sulfoxide (DMSO) was commercially available, dried over calcium hydride, and distilled under reduced pressure. Dimethylformamide (DMF) was dried over phosphorus (V) oxide and distilled before used. The other reagents were used as received.

2.3. Synthesis of p(VDF-*co*-CTFE)-*g*-PAN via SET-LRP process

A typical polymerization of grafted p(VDF-*co*-CTFE)-*g*-PAN via SET-LRP process was carried out as reported [41]. First, 0.5 g of p(VDF-*co*-CTFE) (91/9 mol%) containing 0.6 mmol of Cl atoms was charged into a 50 ml three-necked flask purged with argon. Protected by the inert atmosphere, Cu(0) powder (0.011 g; 0.16 mmol) and Me_6-TREN (0,037 g; 0.16 mmol) or Bpy (0.050 g; 0.3 mmol) were added directly to the flask. The mixture was completely dissolved in DMSO (12.5 ml). After following the addition of acrylonitrile (1,315 g; 24.8 mmol) the reaction mixture was heated at the required temperatures during the required time (Table 1). The resultant p(VDF-*co*-CTFE)-*g*-PAN samples were precipitated in H2O/CH3OH (1/1 vol%) mixture. After filtration and drying, the samples were redissolved in DMF

and reprecipitated in H_2O/CH_3OH (1/1 vol%) mixture. The copolymers were washed with CH_3OH several times and dried at 60 °C for 8 hours under reduced pressure.

2.4. Synthesis of p(VDF-*co*-CTFE)-*g*-PAN via photoinduced Cu(II)-mediated RDRP process

A typical polymerization of grafted p(VDF-*co*-CTFE)-*g*-PAN via photoinduced Cu(II)-mediated RDRP process was carried out as reported [42]. First, 2.5 g of p(VDF-*co*-CTFE) (91/9 mol%) containing 3.2 mmol of Cl atoms was charged into a 100 ml three-necked flask purged with argon. Protected by the inert atmosphere, $CuCl_2$ powder (0.017 g; 0.1 mmol) was added directly to the flask. The mixture was completely dissolved in DMSO (50 ml), then Me_6-TREN (0.139 g; 0.6 mmol) was introduced. After following the addition of acrylonitrile (5.125 g; 96.6 mmol) the reaction mixture was put under the UV light (λ = 365 nm). The resultant samples were taken at the required time (Table 2) and precipitated in H_2O/CH_3OH (1/1 vol%) mixture. After filtration and drying, the samples were redissolved in DMF and reprecipitated in H_2O/CH_3OH (1/1 vol%) mixture. The copolymers were washed with CH_3OH for several times and dried at 60 °C for 8 hours under reduced pressure.

2.5. Synthesis of p(VDF-*co*-TrFE-*co*-CTFE)-*g*-PAN via photoinduced Cu(II)-mediated RDRP process

2.5 g of p(VDF-*co*-TrFE-*co*-CTFE) (80/13/7 mol%) containing 2.4 mmol of Cl atoms was charged into a 100 ml three-necked flask purged with argon. Protected by the inert atmosphere, $CuCl_2$ powder (0.013 g; 0.1 mmol) was added directly to the flask. The mixture was completely dissolved in DMSO (50 ml), then Me_6-TREN (0.102 g; 0.4 mmol) was introduced. After following the addition of acrylonitrile (3.758 g; 70.8 mmol) the reactant mixture was put under the UV light (λ = 365 nm). The resultant samples were taken at the required time (Table 2) and precipitated in H_2O/CH_3OH (1/1 vol%) mixture. After filtration and drying, the samples were redissolved in DMF and reprecipitated in H_2O/CH_3OH (1/1 vol%) mixture. The copolymers were washed with CH_3OH several times and dried at 60 °C for 8 hours under reduced pressure.

2.6. Films fabrication

A typical drop-casting process was used to produce films based on p(VDF-*co*-CTFE)-*g*-PAN and p(VDF-*co*-TrFE-*co*-CTFE)-*g*-PAN copolymers with varied content of grafted PAN. First of all, the copolymers were completely dissolved in DMF by stirring for 12 hours at an elevated temperature. The films were fabricated by casting the solutions obtained onto PTFE evaporating dishes following DMF evaporation at 70 °C. The resultant films with a thickness of 100 μm were peeled off from the PTFE forms.

3. Results and discussion

3.1. Synthesis and chemical structure characterization of PAN-grafted PVDF-based copolymers

SET-LRP process was chosen as an efficient method for the synthesis of grafted p(VDF-*co*-CTFE)-*g*-PAN copolymers (Figure 1a). It has been previously reported that SET-LRP is not only a well-controlled process but also allows avoiding side reactions [41]. In this work, synthetic parameters of SET-LRP process such as a ligand type for catalytic complex formation,

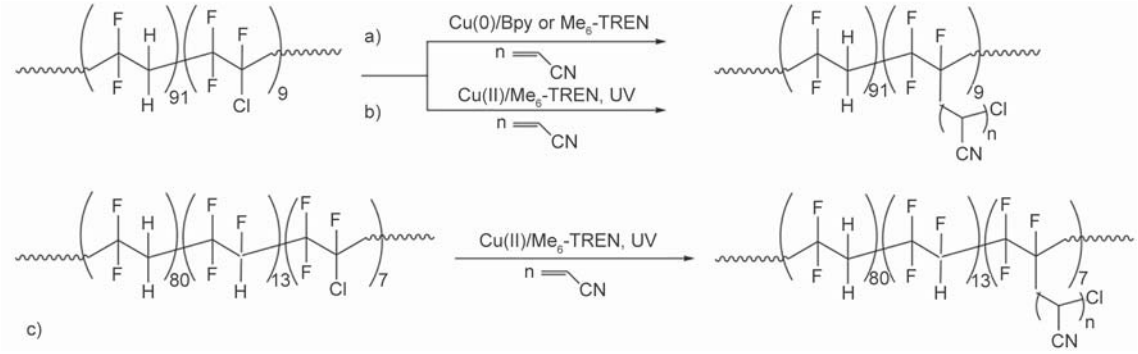

Figure 1. Synthesis of p(VDF-*co*-CTFE)-*g*-PAN via (a) single-electron transfer – living radical polymerization and (b) photoinduced Cu(II)-mediated reversible deactivation radical polymerization (RDRP); (c) synthesis of p(VDF-*co*-TrFE-*co*-CTFE)-*g*-PAN via photoinduced Cu(II)-mediated RDRP.

Table 1. Reaction conditions for the synthesis of p(VDF-*co*-CTFE)-*g*-PAN copolymers with different content of grafted PAN via SET-LRP method.

Batch No.	Catalyst [mmol]	Ligand [mmol]	Reaction temperature [°C]	Reaction time [min]	VDF/CTFE/PAN* [mol%]
Conventional heating					
1	Cu(0), 0.16	Me_6-TREN, 0.16	25	50	91/9/2.5
2	Cu(0), 0.16	Me_6-TREN, 0.16	40	50	91/9/81.4
3	Cu(0), 0.16	Bpy, 0.3	110	50	91/9/29.3
Microwave heating					
4	Cu(0), 0.16	Me_6-TREN, 0.16	40	50	91/9/22.9
5	Cu(0), 0.16	Bpy, 0.3	110	50	91/9/1.3

*PAN content corresponds to additional mol% over 100 mol% of PVDF-based copolymer blocks.

reaction temperature, type of heating (conventional or microwave one) were varied to obtain grafted p(VDF-*co*-CTFE)-*g*-PAN copolymers with different content of grafted PAN (Table 1).

Similar to published grafted PVDF-based polymers [41, 42, 44, 45] the chemical structure of the resultant copolymers was confirmed by a complex of analytical methods including ^{1}H, ^{19}F NMR, and FTIR spectroscopy. It was found that ^{1}H NMR spectroscopy can be used both to confirm the structure of PVDF-based copolymers and to determine the content of grafted PAN. As shown in Figure 2a and Figure 2b, the comparison of pristine p(VDF-*co*-CTFE) with grafted p(VDF-*co*-CTFE)-*g*-PAN copolymer (Batch No.2 in Table 1) shows the change of an integral intensity of the peak at 3.25–3.0 ppm and appearance of a new peak at 2.2–1.8 ppm, which can be utilized to calculate the molar content of grafted PAN [46]. One can see that PAN content corresponds to additional mol% over 100 mol% of PVDF-based copolymer blocks. According to the relevant literature data, the peak at 3.25–3.0 ppm corresponds both to the tail-to-tail connection of VDF and CTFE units and to the proton at the carbon atom nearby a cyano group (Figure 2b signal 2) [41, 42]. A broad new peak appearing at 2.2–1.8 ppm in the spectrum of grafted p(VDF-*co*-CTFE)-*g*-PAN (Figure 2b signal 1) is identified as methylene group proton of PAN chain. Two groups of multiple peaks at 3.0–2.65 ppm and 2.4–2.2 ppm correspond to head-to-tail and tail-to-tail connections of several VDF units. Thus, ^{1}H NMR spectroscopy was utilized to determine the structure of the resultant copolymers and to assign the content of grafted PAN.

^{19}F NMR spectroscopy can be utilized to confirm the structure of grafted p(VDF-*co*-CTFE)-*g*-PAN copolymers. A typical ^{19}F NMR spectrum of original p(VDF-*co*-CTFE) compared to the grafted one is presented in Figure 2c and Figure 2d. It is well-known that the number of peaks around –92 ppm is addressed to a head-to-tail connection of several VDF units while the sequence of peaks around –94, –112, and –120 ppm corresponds to a tail-to-tail connection of VDF and CTFE units [41]. It has been reported that the replacement of chlorine atoms of CTFE units on carbon ones due to the grafting process can be indicated by the appearance of new signals around –113 ppm in ^{19}F NMR spectrum of the grafted copolymers [45]. One can see that a fluorine atom attached to the carbon atom nearby PAN chain appears as a new peak at –112.5 ppm (Figure 2d), which proves the grafting process since this signal is absent in the spectrum of pristine p(VDF-*co*-CTFE) (Figure 2c). In addition, the fact of PAN grafting as a side chain of p(VDF-*co*-CTFE) backbone was confirmed by FTIR spectroscopy since a typical spectrum of grafted p(VDF-*co*-CTFE)-*g*-PAN copolymer has a characteristic absorption band at 2250 cm^{-1} corresponding to a cyano group.

It was proved that SET-LRP method allowed the preparation of grafted copolymers with different content of PAN. Moreover, no side reactions, including typical hydrogenation of CTFE units via transfer metal-catalyzed process were observed. An increase of the reaction temperature was found to promote the grafting process, which gives p(VDF-*co*-CTFE)-*g*-PAN grafted copolymer with a higher content of the incorporated PAN. Besides, utilization

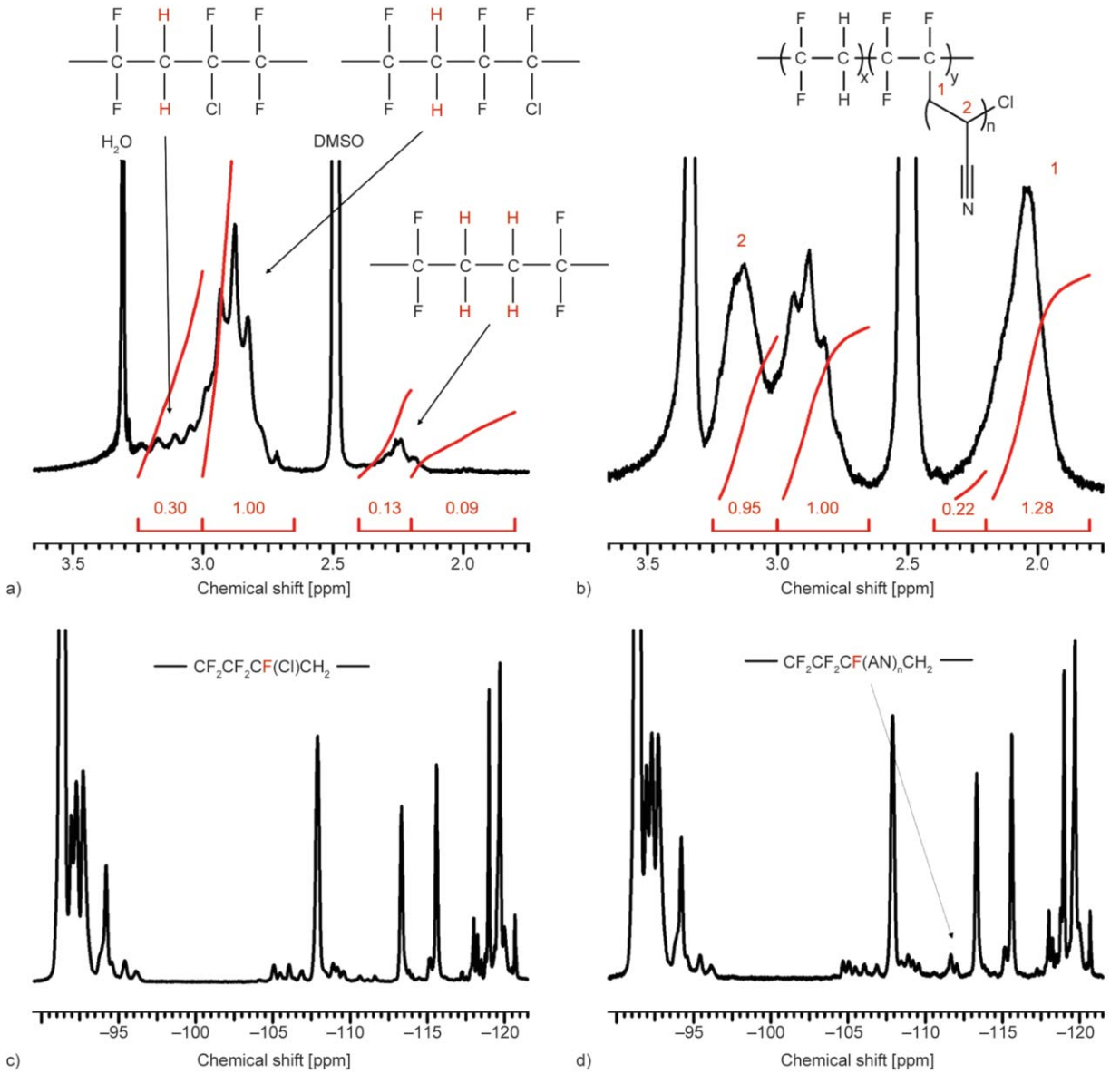

Figure 2. (a) ^{1}H NMR and (c) ^{19}F NMR spectrum of pristine p(VDF-*co*-CTFE) compared to (b) ^{1}H NMR and (d) ^{19}F NMR spectrum of grafted p(VDF-*co*-CTFE)-*g*-PAN (Batch No.2 and Batch No.3 in Table 1).

of tris[2-(dimethylamino)ethyl]amine (Me_6-TREN) as a ligand leads to the production of grafted copolymers with a higher PAN content compared to the reaction at the same conditions but with 2,2′-bipyridine (Bpy) used as a ligand.

In this work, the comparison of microwave and conventional heating applied for SET-LRP method was made for the first time (Table 1). Surprisingly, microwave heating was found to be a less prospective synthetic tool since it gives the copolymers with a lower content of the grafted PAN chains in comparison to conventional ones and requires special equipment.

Despite it was reported that SET-LRP is a well-controlled process for the synthesis of grafted p(VDF-*co*-CTFE)-*g*-PAN copolymers [41], we encountered poor reproducibility of the polymer's characteristics from batch to batch in this work. One can see that SET-LRP requires a higher concentration of the catalytic system as compared to the photoinduced Cu(II)-mediated RDRP process, which can lead to ion metals contamination in the resultant grafted copolymers. Thus, the disadvantages mentioned above stimulated us to search for the other more convenient method of grafted PVDF-based copolymers synthesis. As a result, the photoinduced Cu(II)-mediated RDRP process was chosen as an alternative method of grafted p(VDF-*co*-CTFE)-*g*-PAN and p(VDF-*co*-TrFE-*co*-CTFE)-*g*-PAN copolymers synthesis (Figure 1b, 1c). Unlike SET-LRP process, RDRP proceeds at room temperature under ultraviolet (UV) irradiation

[42, 43]. Moreover, this method seems to be a more rational one since it requires eight times less concentration of a catalytic metal system as compared to the SET-LRP method. Considering further possible applications of the resultant PVDF-based copolymers in electronics, the decrease of catalyst content is a significant advantage.

Applying the method of photoinduced Cu(II)-mediated RDRP polymerization, a series of p(VDF-*co*-CTFE)-*g*-PAN copolymers characterized by different content of the grafted PAN (from 0.6 to 12.7 mol%) was synthesized (Table 2).

It should be noted that another particular benefit of the RDRP method is the controllability of the grafted chain content by simply varying reaction times. The dependence between the reaction time and the grafted PAN content was found to be almost linearly, where PAN content grows with the reaction time increase (Figure 3a). Therefore, it is possible to synthesize a series of grafted p(VDF-*co*-CTFE)-*g*-PAN copolymers

Table 2. Reaction conditions for the synthesis of p(VDF-*co*-CTFE)-*g*-PAN and p(VDF-*co*-TrFE-*co*-CTFE)-*g*-PAN copolymers with different content of the grafted PAN via photoinduced Cu(II)-mediated RDRP method.

Batch No.	Catalyst [mmol]	Ligand [mmol]	Reaction time [min]	VDF/TrFE/CTFE/PAN* [mol%]
p(VDF-*co*-CTFE)-*g*-PAN				
1	Cu(II), 0.02	Me_6-TREN, 0.12	30	91/0/9/0.6
2	Cu(II), 0.02	Me_6-TREN, 0.12	60	91/0/9/2.5
3	Cu(II), 0.02	Me_6-TREN, 0.12	180	91/0/9/5.1
4	Cu(II), 0.02	Me_6-TREN, 0.12	360	91/0/9/8.9
5	Cu(II), 0.02	Me_6-TREN, 0.12	720	91/0/9/12.7
p(VDF-*co*-TrFE-*co*-CTFE)-*g*-PAN				
1	Cu(II), 0.015	Me_6-TREN, 0.09	30	80/13/7/2.7
2	Cu(II), 0.015	Me_6-TREN, 0.09	60	80/13/7/3.5
3	Cu(II), 0.015	Me_6-TREN, 0.09	180	80/13/7/5.4
4	Cu(II), 0.015	Me_6-TREN, 0.09	360	80/13/7/13.5
5	Cu(II), 0.015	Me_6-TREN, 0.09	720	80/13/7/14.5

*PAN content corresponds to additional mol% over 100 mol% of PVDF-based copolymer blocks.

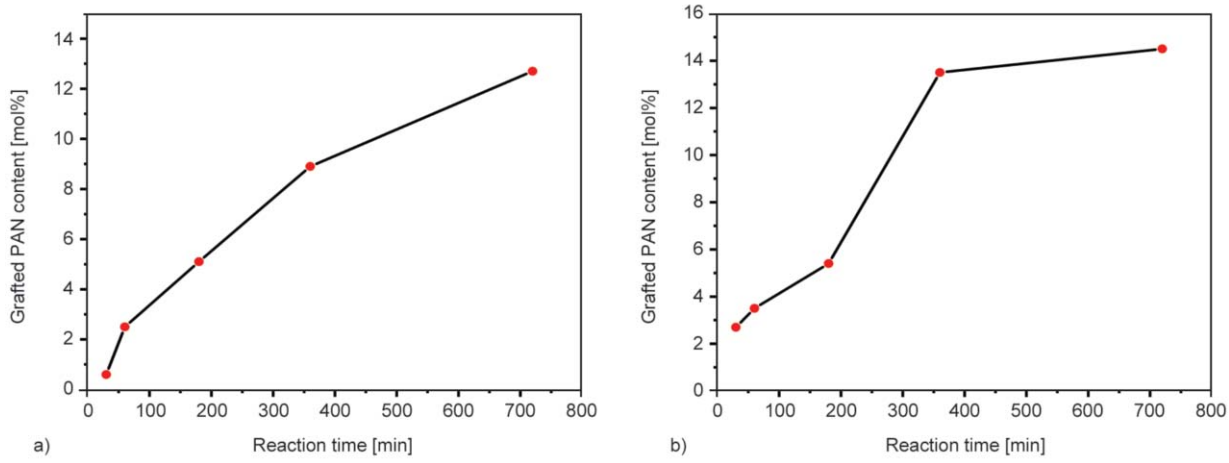

Figure 3. The influence of the reaction time on the content of polyacrylonitrile grafted onto the side chains of (a) p(VDF-*co*-CTFE) and (b) p(VDF-*co*-TrFE-*co*-CTFE) (Table 2).

with a desirable content of PAN chains and then to investigate the structure-properties relationship of all of them.

Considering the obvious advantages of the photoinduced Cu(II)-mediated polymerization, this method was utilized to synthesize the series of grafted p(VDF-*co*-TrFE-*co*-CTFE)-*g*-PAN copolymers with varying PAN content (Table 2). Synthetic reaction parameters for the grafted copolymers p(VDF-*co*-CTFE)-*g*-PAN preparation were simply adapted to synthesize p(VDF-*co*-TrFE-*co*-CTFE)-*g*-PAN using the same ratio of chlorine atoms to Cu(II)/Me_6-TREN and to acrylonitrile monomer. The content of grafted PAN was also controlled by varying the reaction time. It has been expected that a similar impact of the reaction time to PAN content as for synthesized p(VDF-*co*-CTFE)-*g*-PAN copolymers would be revealed. However, PAN content increased intensely at low reaction time (from 2.7 to 13.5 mol% up to 360 minutes) and practically did not change for a longer reaction time (Figure 3b). In comparison to p(VDF-*co*-CTFE) the rate of PAN grafting to p(VDF-*co*-TrFE-*co*-CTFE) backbone at the elevated reaction time was reduced more pronounced, which can be attributed to a feature of the molecular conformation of the latter polymer, which impacts the rate of the polymerization. It was shown that the content of grafted copolymer could be promoted by extending the reaction time or increase of either monomer or ligand ratio to chlorine atoms [42, 43].

3.2. Phase behavior and thermal properties of PAN-grafted PVDF-based copolymers

Phase behavior and thermal stability of the grafted p(VDF-*co*-CTFE)-*g*-PAN and p(VDF-*co*-TrFE-*co*-CTFE)-*g*-PAN copolymers synthesized via photoinduced Cu(II)-mediated RDRP process were investigated by differential scanning calorimetry (DSC) and thermogravimetric analysis (TGA) methods. The phase behavior investigation of the series of grafted p(VDF-*co*-CTFE)-*g*-PAN and p(VDF-*co*-TrFE-*co*-CTFE)-*g*-PAN copolymers in comparison to pristine ones allowed to reveal some crucial dependences. A declining trend for both melting temperature (T_m) and melting enthalpy (ΔH_m) values with an increase of the grafted PAN content was observed (Figure 4 and Table 3). The melting enthalpy decline accompanied by the increase of PAN content

Table 3. The impact of PAN content on the melting temperature and enthalpy of grafted p(VDF-*co*-CTFE)-*g*-PAN and p(VDF-*co*-TrFE-*co*-CTFE)-*g*-PAN compared to pristine ones.

VDF/CTFE/PAN	T_m [°C]	ΔH_m [J/g]	VDF/TrFE/CTFE/PAN	T_m [°C]	ΔH_m [J/g]
91/9/0	167.0	–14.8	80/13/7/0	122.0	–17.4
91/9/0.6	169.7	–13.4	80/13/7/2.7	125.6	–14.2
91/9/2.5	168.8	–13.3	80/13/7/3.5	124.7	–14.0
91/9/5.1	164.3	–13.2	80/13/7/5.4	119.0	–12.7
91/9/8.9	165.0	–11.5	80/13/7/13.5	118.0	–11.3
91/9/12.7	165.0	–11.2	80/13/7/14.5	117.4	–10.5

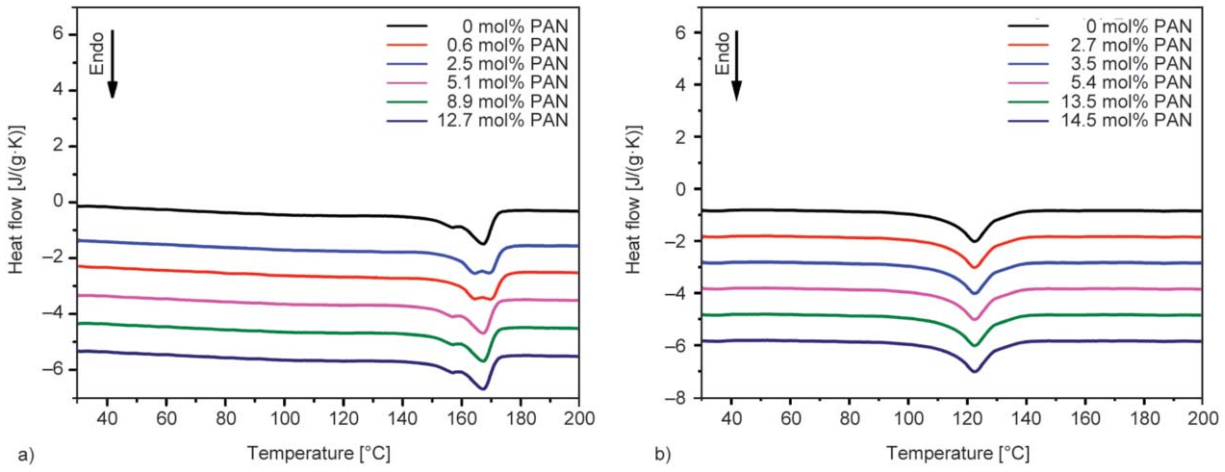

Figure 4. DSC scans of (a) p(VDF-*co*-CTFE)-*g*-PAN and (b) p(VDF-*co*-TrFE-*co*-CTFE)-*g*-PAN with different content of grafted PAN.

indirectly indicates a decrease of crystallinity due to the appearance of grafted bulky and amorphous PAN segments.

The impact of PAN content grafted onto the side chains of p(VDF-*co*-CTFE) on the thermal stability of the resultant copolymers was investigated using TGA analysis (Figure 5a, 5b).

As shown in Figure 5a, the pristine p(VDF-*co*-CTFE) begins to decompose in the air at a temperature of about 400 °C while the grafted copolymers demonstrate two degradation stages. The first stage of p(VDF-*co*-CTFE)-*g*-PAN degradation is attributed to PAN segment decomposition and assigned to the temperature of about 370 °C. Another decomposition stage at 400 °C corresponds to the degradation of p(VDF-*co*-CTFE) macromolecular chain. It has been observed that at the temperature of 500 °C the residual weight enhances with the increasing of the grafted PAN content in p(VDF-*co*-CTFE)-*g*-PAN copolymers. It can be explained by the carbonization of PAN segments into polycyclic compounds characterized with higher thermal stability under thermal oxidation conditions [47]. The results of TGA analysis at the inert atmosphere (Figure 5b) confirm the trend of the residual weight increase with PAN content enhance. Moreover, PAN segments do not depredate completely under the inert atmosphere up to the temperature of 700 °C. To summarize, the results of TGA analysis show that the grafted copolymers are thermally less stable than pristine p(VDF-*co*-CTFE) copolymer.

However, investigation of the thermal properties of pristine p(VDF-*co*-TrFE-*co*-CTFE) and grafted p(VDF-*co*-TrFE-*co*-CTFE)-*g*-PAN copolymers showed that grafting leads to an increase of the decomposition temperature from 360 °C for the pristine copolymer to 410–420 °C for the grafted copolymers (Figure 5c). Moreover, it was confirmed that an

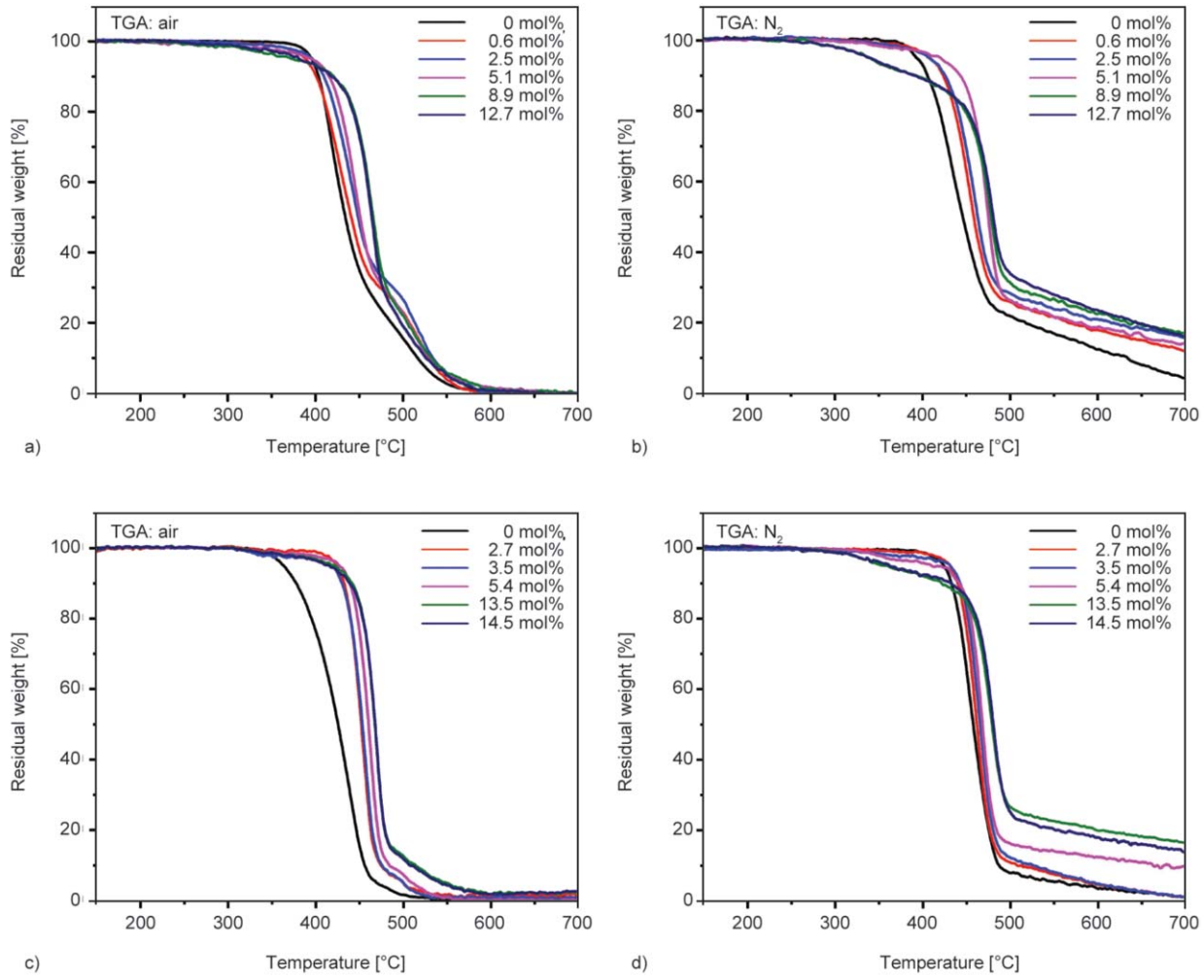

Figure 5. TGA curves of p(VDF-*co*-CTFE)-*g*-PAN and p(VDF-*co*-TrFE-*co*-CTFE)-*g*-PAN with different content of grafted PAN (a) and (c) in air; (b) and (d) under an inert atmosphere.

increase of the PAN content leads to residual weight enhance (Figure 5d). Hence, the changes of thermal stability of the grafted copolymers in comparison to the pristine PVDF-based copolymers confirm that PAN segments were successfully grafted via photoinduced Cu(II)-mediated RDRP process.

3.3. Dielectric properties of PAN-grafted PVDF-based copolymers

The dielectric properties of grafted p(VDF-*co*-CTFE)-*g*-PAN and p(VDF-*co*-TrFE-*co*-CTFE)-*g*-PAN copolymers with different content of PAN synthesized via photoinduced Cu(II)-mediated RDRP process were investigated. First of all, the dielectric constant as a function of frequency was measured at room temperature and low electric field (1 V) (Figure 6a, 6b).

It has been found that the incorporation of PAN onto the side chains of pristine p(VDF-*co*-CTFE) has a significant impact on the dielectric properties since it leads to an increasing dielectric constant for all the grafted copolymers. It has been measured that pristine p(VDF-*co*-CTFE) has a dielectric constant about 2.0 (at a standard frequency of 10^2 Hz). Meanwhile grafted p(VDF-*co*-CTFE)-*g*-PAN copolymer containing 0.6 mol% of PAN has a dielectric constant of about 4.5 at the same frequency, which is twice larger than for pristine one. Apparently, further growth of the grafted PAN content leads to a decline of the dielectric constant, which still remains higher compared to the dielectric constant of pristine p(VDF-*co*-CTFE). Since the increase of the reaction time causes growth of PAN content for the grafted copolymers synthesized via RDRP process, it might be suggested that metal ions contamination in the resultant grafted copolymers increases at the same time. Thus, the reduction of the dielectric constant with further increase of PAN content might be attributed to the impact of metal ions contamination in the resultant grafted copolymers, which can significantly affect their dielectric properties.

The dielectric constant of p(VDF-*co*-TrFE-*co*-CTFE)-*g*-PAN copolymers were measured to reveal PAN grafting's impact on the dielectric properties. As it turned out, the incorporation of PAN chains allows obtaining the materials with the dielectric constant almost twice higher as compared to pristine p(VDF-*co*-TrFE-*co*-CTFE). As shown in Figure 6b, p(VDF-*co*-TrFE-*co*-CTFE) demonstrates the dielectric constant 7.0 at the frequency of 10^2 Hz, while grafted ones (containing 2.7 and 3.5 mol% of PAN) have the dielectric constant around 15.0 at the same frequency.

Further comparison of the dielectric properties of p(VDF-*co*-CTFE)-*g*-PAN and p(VDF-*co*-TrFE-*co*-CTFE)-*g*-PAN copolymers with different content of PAN show that grafted copolymers based on p(VDF-*co*-TrFE-*co*-CTFE) have conductivity one order of magnitude higher than those based on p(VDF-*co*-CTFE) (Figure 6c, 6d). It is also the evidence that conductivity varies over a decade within the concentration range for copolymers p(VDF-*co*-TrFE-*co*-CTFE)-*g*-PAN, while for grafted copolymers p(VDF-*co*-CTFE)-*g*-PAN, this variation is around 3 times. It should be noted that the frequency dependence of the conductivity for both types of copolymers follows the universal dielectric response behavior, which is typical for hopping conduction in a heterogeneous systems [48]. The effect of conductivity is also manifested in the frequency dependence of the dielectric loss, especially in the low frequency range, below 10 Hz (Figure 6e, 6f). It should be noted that for grafted copolymers based on p(VDF-*co*-TrFE-*co*-CTFE) dielectric loss is 1.5 decades higher than for p(VDF-*co*-CTFE)-*g*-PAN copolymers.

The distance between hopping sites can be qualitatively estimated from the frequency dependence of imaginary electric modulus M'' (see Figure 7a, 7b). The presence of a maximum in such dependence corresponds to a change in the slope of the frequency dependence of conductivity, *i.e.*, transition to bulk conductance in the system. It is clear that in grafted copolymers based on p(VDF-*co*-TrFE-*co*-CTFE), this transition occurs at a much higher frequency than in p(VDF-*co*-CTFE)-*g*-PAN copolymers. Accordingly, the distance between hopping sites is smaller in grafted p(VDF-*co*-TrFE-*co*-CTFE)-*g*-PAN copolymers.

The effect of conductivity is clearly visible in Cole-Cole diagrams for both types of grafted copolymers (Figure 7c, 7d). The low frequency 'tail' is much more evident in p(VDF-*co*-TrFE-*co*-CTFE)-*g*-PAN copolymers, making the semicircle of the main dielectric relaxation almost invisible in the appropriate loss axis scale.

Hence, the changes in the dielectric performance of the grafted copolymers compared to pristine ones could be used to develop material with required dielectric characteristics, which is advantageous for further electronic applications.

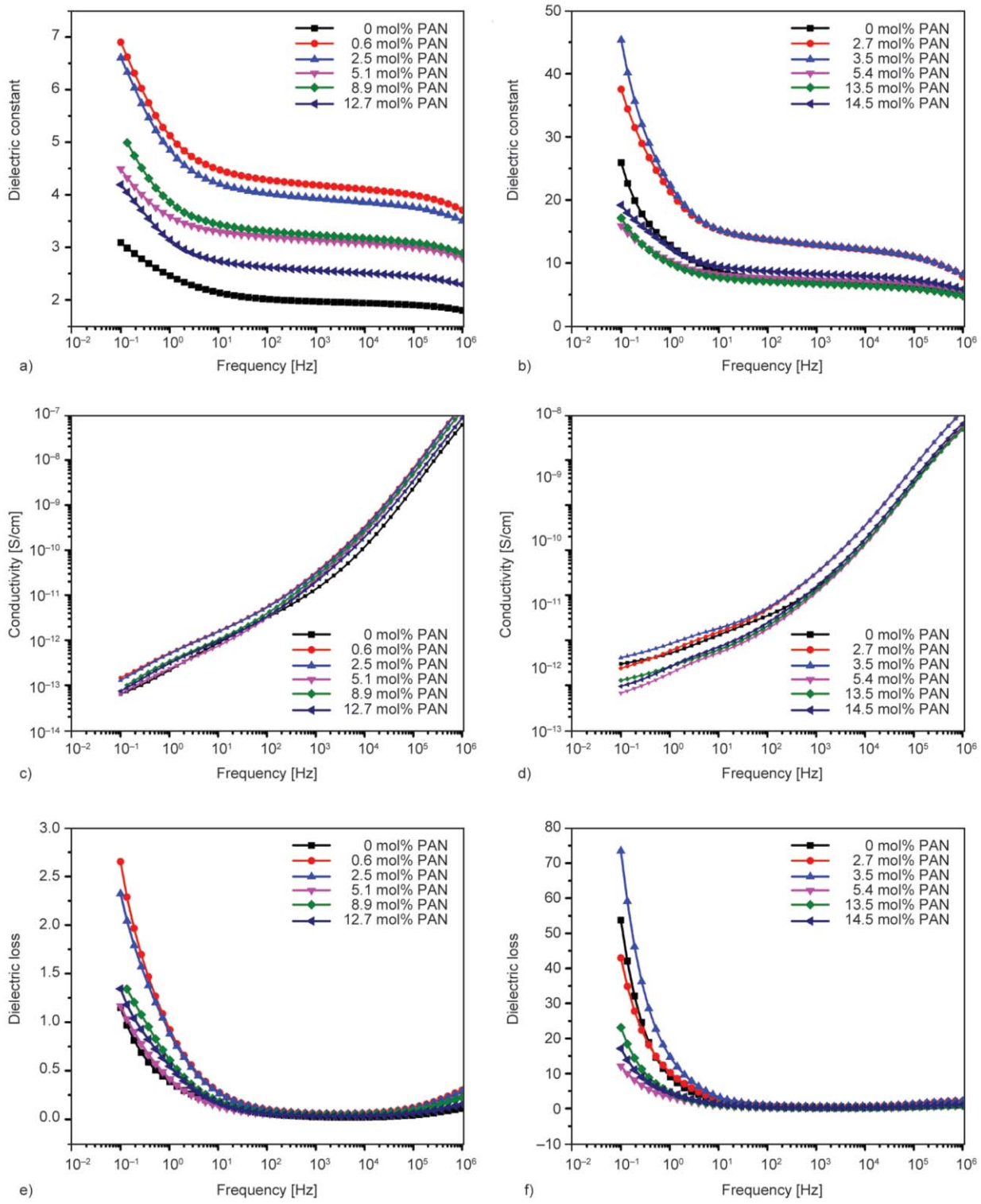

Figure 6. The dielectric constant as a function of frequency for (a) p(VDF-*co*-CTFE)-*g*-PAN and (b) p(VDF-*co*-TrFE-*co*-CTFE)-*g*-PAN with different content of grafted PAN. The conductivity as a function of frequency for (c) p(VDF-*co*-CTFE)-*g*-PAN and (d) p(VDF-*co*-TrFE-*co*-CTFE)-*g*-PAN with different content of grafted PAN. The dielectric loss as a function of frequency for (e) p(VDF-*co*-CTFE)-*g*-PAN and (f) p(VDF-*co*-TrFE-*co*-CTFE)-*g*-PAN with different content of grafted PAN.

4. Conclusions

In summary, p(VDF-*co*-CTFE)-*g*-PAN copolymers with different content of grafted PAN chains were synthesized via single electron transfer radical polymerization (utilizing microwave or conventional heating) and photoinduced Cu(II)-mediated reversible deactivation radical polymerization processes. The benefits and drawbacks of two different strategies

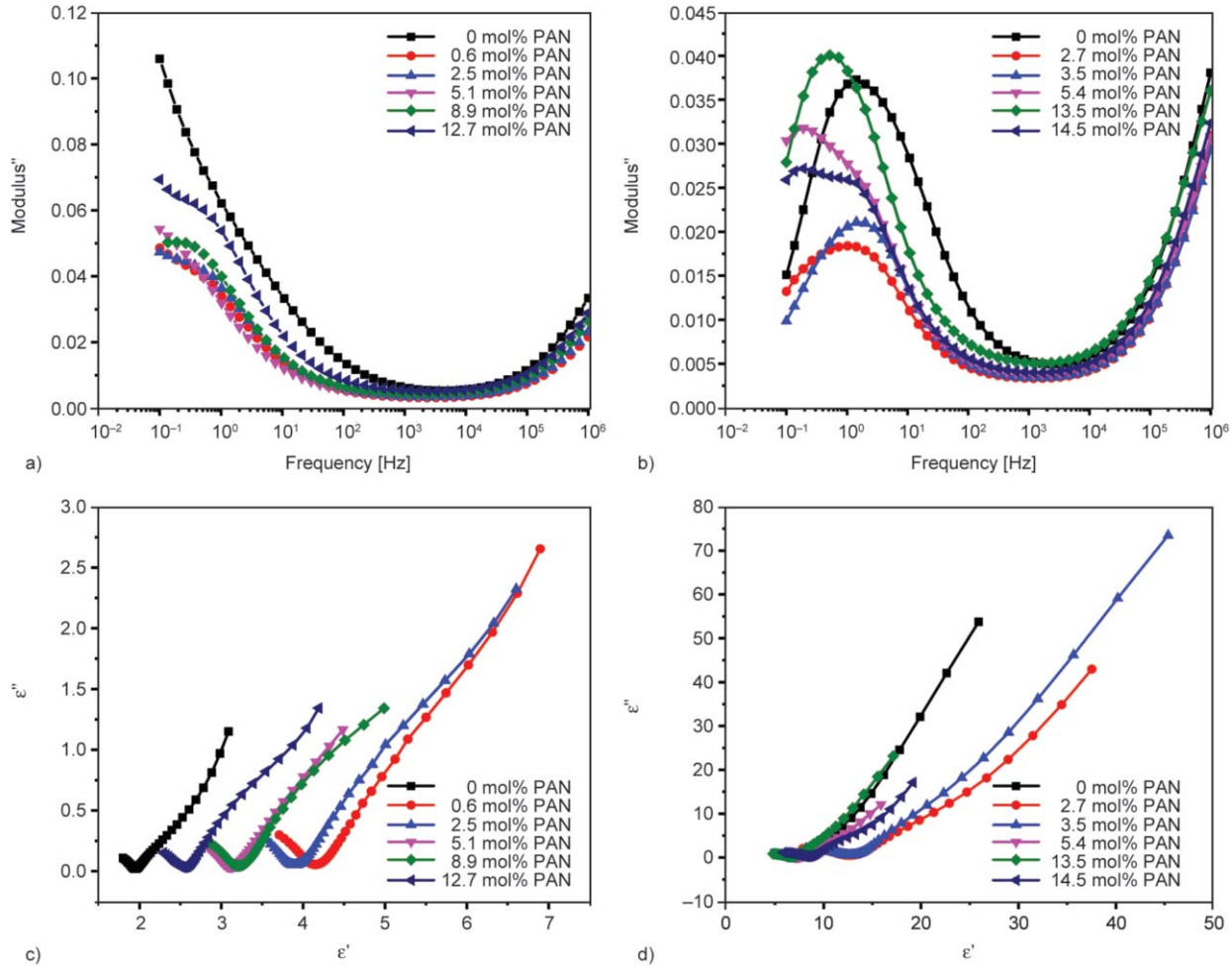

Figure 7. The imaginary electric modulus as a function of frequency of (a) p(VDF-*co*-CTFE)-*g*-PAN and (b) p(VDF-*co*-TrFE-*co*-CTFE)-*g*-PAN and the Cole-Cole diagrams of (c) p(VDF-*co*-CTFE)-*g*-PAN and (d) p(VDF-*co*-TrFE-*co*-CTFE)-*g*-PAN with different content of grafted PAN.

for p(VDF-*co*-CTFE)-*g*-PAN grafted copolymers synthesis were compared and discussed for the first time. Considering the benefits of the photoinduced RDRP process, such as reduced metal catalytic system concentration and well controllability of the incorporated PAN content, it was employed to prepare a series of novel p(VDF-*co*-TrFE-*co*-CTFE)-*g*-PAN copolymers. Investigation of phase behavior, thermal stability, and dielectric properties of p(VDF-*co*-CTFE)-*g*-PAN and p(VDF-*co*-TrFE-*co*-CTFE)-*g*-PAN copolymers synthesized allowed revealing the impact of polymer backbone composition and the grafted PAN content on these properties. This is the first systematic investigation of the dielectric properties of PAN-grafted PVDF-based copolymers. It was shown that PAN grafting onto PVDF-based copolymers backbone leads to crucial dielectric properties changes since the dielectric constant of the polyacrylonitrile-grafted copolymers was twice enhanced as compared to the pristine copolymers. One can see that tuning the dielectric properties of grafted PVDFt-based copolymers containing a varied amount of incorporated PAN can be used to develop materials with required dielectric properties for further electronic applications.

Acknowledgements

This work was financially supported by the Russian Science Foundation (grant 19-73-30028). Registration of NMR and FTIR spectra was performed on the equipment of the Collaborative Access Center 'Center for Polymer Research' of ISPM RAS under financial support from the Ministry of Science and Higher Education of the Russian Federation (Contract 0071-2019-0006).

References

[1] Wall L. A.: Fluoropolymers. Wiley-Interscience, New York (1972).

[2] Banks R. E., Smart B. E., Tatlow J. C.: Organofluorine chemistry: Principles and commercial applications. Springer, New York (1994).

[3] Scheirs J.: Modern fluoropolymers: High performance polymers for diverse applications. Wiley, New York (1997).

[4] Chu B., Zhou X., Ren K., Neese B., Lin M., Wang Q., Bauer F., Zhang Q. M.: A dielectric polymer with high electric energy density and fast discharge speed. Science, **313**, 334–336 (2006). https://doi.org/10.1126/science.1127798

[5] Persano L., Dagdeviren C., Su Y., Zhang Y., Girardo S., Pisignano D., Huang Y., Rogers J. A.: High performance piezoelectric devices based on aligned arrays of nanofibers of poly(vinylidenefluoride-*co*-trifluoroethylene). Nature Communications, **4**, 1633/1–1633/10 (2013). https://doi.org/10.1038/ncomms2639

[6] Katsouras I., Asadi K., Li M., van Driel T. B., Kjær K. S., Zhao D., Lenz T., Gu Y., Blom P. W. M., Damjanovic D., Nielsen M. M., de Leeuw D. M.: The negative piezoelectric effect of the ferroelectric polymer poly(vinylidene fluoride). Nature Materials, **15**, 78–84 (2016). https://doi.org/10.1038/nmat4423

[7] Hougham G. G., Cassidy P. E., Johns K., Davidson T.: Fluoropolymers 2: Properties. Springer, New York (1999).

[8] Améduri B., Boutevin B.: Well-architectured fluoropolymers: Synthesis, properties and applications. Elsevier, Amsterdam (2004).

[9] Améuri B., Boutevin B., Kostov G.: Fluoroelastomers: Synthesis, properties and applications. Progress in Polymer Science, **26**, 105–187 (2001). https://doi.org/10.1016/S0079-6700(00)00044-7

[10] Ameduri B.: From vinylidene fluoride (VDF) to the applications of VDF-containing polymers and copolymers: Recent developments and future trends. Chemical Reviews, **109**, 6632–6686 (2009). https://doi.org/10.1021/cr800187m

[11] Zhang X., Zhang C., Lin Y., Hu P., Shen Y., Wang K., Meng S., Chai Y., Dai X., Liu X., Liu Y., Mo X., Cao C., Li S., Deng X., Chen L.: Nanocomposite membranes enhance bone regeneration through restoring physiological electric microenvironment. ACS Nano, **10**, 7279–7286 (2016). https://doi.org/10.1021/acsnano.6b02247

[12] Han X., Chen X., Tang X., Chen Y-L., Liu J-H., Shen Q-D.: Flexible polymer transducers for dynamic recognizing physiological signals. Advanced Functional Materials, **26**, 3640–3648 (2016). https://doi.org/10.1002/adfm.201600008

[13] Yu K., Bai Y., Zhou Y., Niu Y., Wang H.: Poly(vinylidene fluoride) polymer based nanocomposites with enhanced energy density by filling with polyacrylate elastomers and $BaTiO_3$ nanoparticles. Applied Physics Letters, **104**, 082904/1–082904/4 (2014). https://doi.org/10.1063/1.4866585

[14] Zhang Z., Chung T. C. M.: Study of VDF/TrFE/CTFE terpolymers for high pulsed capacitor with high energy density and low energy loss. Macromolecules, **40**, 783–785 (2007). https://doi.org/10.1021/ma0627119

[15] Kepler R. G.: Ferroelectric, pyroelectric, and piezoelectric properties of poly(vinylidene fluoride). in 'Ferroelectric polymers' (ed.: H. S. Nalwa) Marcel Dekker, New York, 63–180 (1995).

[16] Stadlober B., Zirkl M., Irimia-Vladu M.: Route towards sustainable smart sensors: Ferroelectric polyvinylidene fluoride-based materials and their integration in flexible electronics. Chemical Society Reviews, **48**, 1787–1825 (2019). https://doi.org/10.1039/C8CS00928G

[17] Gaur A. M., Rana D. S.: *In situ* measurement of dielectric permittivity and electrical conductivity of $CoCl_2$/$BaCl_2$ doped PVDF composite at elevated temperature, **29**, 1637–1644 (2019). https://doi.org/10.1007/s10904-019-01126-y

[18] Park J. H., Kurra N., AlMadhoun M. N., Odeh I. N., Alshareef H. N.: A two-step annealing process for enhancing the ferroelectric properties of poly(vinylidene fluoride) (PVDF) devices. Journal of Materials Chemistry C, **3**, 2366–2370 (2015). https://doi.org/10.1039/C4TC02079K

[19] Satapathy S., Pawar S., Gupta P. K., Varma K. B. R.: Effect of annealing on phase transition in poly(vinylidene fluoride) films prepared using polar solvent. Bulletin of Materials Science, **34**, 727/1–727/7 (2011). https://doi.org/10.1007/s12034-011-0187-0

[20] Lopes A. C., Gutiérrez J., Barandiarán J. M.: Direct fabrication of a 3D-shape film of polyvinylidene fluoride (PVDF) in the piezoelectric β-phase for sensor and actuator applications. European Polymer Journal, **99**, 111–116 (2018). https://doi.org/10.1016/j.eurpolymj.2017.12.009

[21] Almadhoun M. N., Khan M. A., Rajab K., Park J. H., Buriak J. M., Alshareef H. N.: UV-induced ferroelectric phase transformation in PVDF thin films. Advanced Electronic Materials, **5**, 1800363/1–1800363/6 (2018). https://doi.org/10.1002/aelm.201800363

[22] Wang J., Li Z., Yan Y., Wang X., Xie Y-C., Zhang Z-C.: Improving ferro- and piezo-electric properties of hydrogenized poly(vinylidene fluoride-trifluoroethylene) films by annealing at elevated temperatures. Chinese Journal of Polymer Science, **34**, 649–658 (2016). https://doi.org/10.1007/s10118-016-1782-8

[23] Tan S., Liu E., Zhang Q., Zhang Z.: Controlled hydrogenation of P(VDF-*co*-CTFE) to prepare P(VDF-*co*-TrFE-*co*-CTFE) in the presence of CuX (X = Cl, Br) complexes. Chemical Communications, **47**, 4544–4546 (2011). https://doi.org/10.1039/C1CC00106J

[24] Lu Y., Claude J., Zhang Q., Wang Q.: Microstructures and dielectric properties of the ferroelectric fluoropolymers synthesized *via* reductive dechlorination of poly (vinylidene fluoride-*co*-chlorotrifluoroethylene)s. Macromolecules, **39**, 6962–6968 (2006). https://doi.org/10.1021/ma061311i

[25] Chu H., Fu C., Wu X., Tan Z., Qian J., Li W., Ran X., Nie W.: Enhancing released electrical energy density of poly(vinylidene fluoride-*co*-trifluoroethylene)-graft-poly (methyl methacrylate) *via* the pre-irradiation method. Applied Surface Science, **465**, 643–655 (2019). https://doi.org/10.1016/j.apsusc.2018.08.222

[26] Wang J., Xie Y., Liu J., Zhang Z., Zhang Y.: Towards high efficient nanodielectrics from linear ferroelectric P(VDF-TrFE-CTFE)-*g*-PMMA matrix and exfoliated mica nanosheets. Applied Surface Science, **469**, 437–445 (2019). https://doi.org/10.1016/j.apsusc.2018.11.073

[27] Tan S., Xiong J., Zhao Y., Liu J., Zhang Z.: Synthesis of poly(vinylidene fluoride-*co*-chlorotrifluoroethylene)-*g*-poly(methyl methacrylate) with low dielectric loss by photo-induced metal-free ATRP. Journal of Materials Chemistry C, **6**, 4131–4139 (2018). https://doi.org/10.1039/C8TC00781K

[28] Li J., Hu X., Gao G., Ding S., Li H., Yang L., Zhang Z.: Tuning phase transition and ferroelectric properties of poly(vinylidene fluoride-*co*-trifluoroethylene) *via* grafting with desired poly(methacrylic ester)s as side chains. Journal of Materials Chemistry C, **1**, 1111–1121 (2013). https://doi.org/10.1039/C2TC00431C

[29] Miao B., Liu J., Zhang X., Lu J., Tan S., Zhang Z.: Ferroelectric relaxation dependence of poly(vinylidene fluoride-*co*-trifluoroethylene) on frequency and temperature after grafting with poly(methyl methacrylate). RSC Advances, **6**, 84426–84438 (2016). https://doi.org/10.1039/C6RA17977K

[30] Li Z., Wang Y., Cheng Z-Y.: Electromechanical properties of poly(vinylidene-fluoride-chlorotrifluoroethylene) copolymer. Applied Physics Letters, **88**, 062904/1–062904/3 (2006). https://doi.org/10.1063/1.2170425

[31] Liu Y., Lee J. Y., Kang E. T., Wang P., Tan K. L.: Synthesis, characterization and electrochemical transport properties of the poly(ethyleneglycol)–grafted poly-(vinylidenefluoride) nanoporous membranes. Reactive and Functional Polymers, **47**, 201–213 (2001). https://doi.org/10.1016/S1381-5148(01)00030-X

[32] Liu Y., Lee J. Y., Hong L.: Synthesis, characterization and electrochemical properties of poly(methyl methacrylate)-grafted-poly(vinylidene fluoride-hexafluoropropylene) gel electrolytes. Solid State Ionics, **150**, 317–326 (2002). https://doi.org/10.1016/S0167-2738(02)00523-4

[33] Zhang M., Russell T. P.: Graft copolymers from poly (vinylidene fluoride-*co*-chlorotrifluoroethylene) *via* atom transfer radical polymerization. Macromolecules, **39**, 3531–3539 (2006). https://doi.org/10.1021/ma060128m

[34] Sun S. W., Gao X. L.: Preparation of a PVDF/PVDF-*g*-(PSSS-*co*-PAA) graft copolymerization-blending cation exchange material and effects of the synthesis method on the material structures and properties. Express Polymer Letters, **15**, 39–44 (2021). https://doi.org/10.3144/expresspolymlett.2021.5

[35] Dünki S. J., Nüesch F. A., Opris D. M.: Elastomers with tunable dielectric and electromechanical properties. Journal of Materials Chemistry C, **4**, 10545–10553 (2016). https://doi.org/10.1039/C6TC01731B

[36] Wang J-S., Matyjaszewski K.: Controlled/'living' radical polymerization. Atom transfer radical polymerization in the presence of transition-metal complexes. Journal of the American Chemical Society, **117**, 5614–5615 (1995). https://doi.org/10.1021/ja00125a035

[37] Kato M., Kamigaito M., Sawamoto M., Higashimura T.: Polymerization of methyl methacrylate with the carbon tetrachloride/dichlorotris-(triphenylphosphine)ruthenium(II)/methylaluminum bis(2,6-di-tert-butylphenoxide) initiating system: Possibility of living radical polymerization. Macromolecules, **28**, 1721–1723 (1995). https://doi.org/10.1021/ma00109a056

[38] Patten T. E., Xia J., Abernathy T., Matyjaszewski K.: Polymers with very low polydispersities from atom transfer radical polymerization. Science, **272**, 866–868 (1996). https://doi.org/10.1126/science.272.5263.866

[39] Matyjaszewski K., Xia J.: Atom transfer radical polymerization. Chemical Reviews, **101**, 2921–2990 (2001). https://doi.org/10.1021/cr940534g

[40] Singha N. K., Mays J.: Reversible deactivation radical polymerization: Synthesis and applications of functional polymers. De Gruyter, Berlin (2020). https://doi.org/10.1515/9783110643695

[41] Hu X., Li J., Li H., Zhang Z.: Synthesis and characterization of poly(vinylidene fluoride-*co*-chlorotrifluoroethylene)-grafted-poly(acrylonitrile) *via* single electron transfer–living radical polymerization process. Journal of Polymer Science Part A: Polymer Chemistry, **50**, 3126–3134 (2012). https://doi.org/10.1002/pola.26099

[42] Hu X., Cui G., Zhu N., Zhai J., Guo K.: Photoinduced Cu(II)-mediated RDRP to P(VDF-*co*-CTFE)-*g*-PAN. Polymers, **10**, 68/1–68/10 (2018). https://doi.org/10.3390/polym10010068

[43] Hu X., Cui G., Zhang Y., Zhu N., Guo K.: Copper(II) photoinduced graft modification of P(VDF-*co*-CTFE). European Polymer Journal, **100**, 228–232 (2018). https://doi.org/10.1016/j.eurpolymj.2018.01.033

[44] Hsu C-Y., Liu R-J., Hsu C-H., Kuo P-L.: High thermal and electrochemical stability of PVDF-*graft*-PAN copolymer hybrid PEO membrane for safety reinforced lithium-ion battery. RSC Advances, **6**, 18082–18088 (2016). https://doi.org/10.1039/C5RA26345J

[45] Eken G. A., Acar M. H.: PVDF-based shape memory polymers. European Polymer Journal, **114**, 249–254 (2019). https://doi.org/10.1016/j.eurpolymj.2019.02.040

[46] Zhu N., Hu X., Zhang Y., Zhang K., Li Z., Guo K.: Continuous flow SET-LRP in the presence of P(VDF-*co*-CTFE) as macroinitiator in a copper tubular reactor. Polymer Chemistry, **7**, 474–480 (2016). https://doi.org/10.1039/C5PY01728A

[47] Yusof N., Ismail A. F.: Polyacrylonitrile/acrylamide-based carbon fibers prepared using a solvent-free coagulation process: Fiber properties and its structure evolution during stabilization and carbonization. Polymer Engineering and Science, **52**, 360–366 (2011). https://doi.org/10.1002/pen.22090

[48] Dyre J. C., Schrøder T. B.: Universality of ac conduction in disordered solids. Reviews of Modern Physics, **72**, 873–892 (2000). https://doi.org/10.1103/RevModPhys.72.873